Residual drift analyses of realistic self-centering concrete wall systems

Richard S. Henry[*1], Sri Sritharan[2a] and Jason M. Ingham[1b]

[1]*Department Civil and Environmental Engineering, University of Auckland, New Zealand*
[2]*Department Civil, Construction, and Environmental Engineering, Iowa State University, Ames, IA, USA*

Abstract. To realise the full benefits of a self-centering seismic resilient system, the designer must ensure that the entire structure does indeed re-center following an earthquake. The idealised flag-shaped hysteresis response that is often used to define the cyclic behaviour of self-centering concrete systems seldom exists and the residual drift of a building subjected to an earthquake is dependent on the realistic cyclic hysteresis response as well as the dynamic loading history. Current methods that are used to ensure that re-centering is achieved during the design of self-centering concrete systems are presented, and a series of cyclic analyses are used to demonstrate the flaws in these current procedures, even when idealised hysteresis models were used. Furthermore, results are presented for 350 time-history analyses that were performed to investigate the expected residual drift of an example self-centering concrete wall system during an earthquake. Based upon the results of these time-history analyses it was concluded that due to dynamic shake-down the residual drifts at the conclusion of the ground motion were significantly less than the maximum possible residual drifts that were observed from the cyclic hysteresis response, and were below acceptable residual drift performance limits established for seismic resilient structures. To estimate the effect of the dynamic shake-down, a residual drift ratio was defined that can be implemented during the design process to ensure that residual drift performance targets are achieved for self-centering concrete wall systems.

Keywords: residual drift; self-centering; unbonded post-tensioning; precast concrete; shear walls; seismic response

1. Introduction

The main objective of seismic resilient design is to safely dissipate the energy imparted to a structure during an earthquake with minimal structural damage. Given the difficulty in straightening a building which is left with a significant residual drift following an earthquake, self-centering behaviour is a critical aspect of seismic resilient design. Self-centering structural precast concrete components that utilise unbonded post-tensioning (PT) were initially developed during the PRESSS research program (Priestley *et al.* 1999). The behaviour of self-centering concrete

---

*Corresponding author, Ph.D., E-mail: rs.henry@auckland.ac.nz
[a]Professor, E-mail: sri@iastate.edu
[b]Professor, E-mail: j.ingham@auckland.ac.nz

systems is often characterised by a flag-shaped hysteresis response. However, when an idealised flag-shaped cyclic hysteresis response is used to define the self-centering behaviour of PT concrete structures, three major factors are ignored. First, in reality the response of a concrete member with unbonded PT does not follow a perfect bilinear-elastic hysteresis rule as an imperfect flag-shape and small residual displacements are often observed. Second, the influence that other structural and non-structural elements have on the hysteresis response of the entire system is ignored. Third, investigation of a pushover or cyclic hysteresis response does not account for the dynamic shake-down that occurs following the structure experiencing a few high-intensity displacement cycles during an earthquake.

2. Background

2.1 Hysteresis response of self-centering systems

The response of a self-centering concrete system is typically characterised by a flag-shaped hysteresis loop. For a concrete member with unbonded PT, the hysteresis response is often assumed to be bi-linear elastic, with zero residual displacement. The combination of the bi-linear elastic response and the elasto-plastic response of the energy dissipating components results in the idealised flag-shape response, as shown in Fig. 1.

Based on the ideal flag-shape shown in Fig. 1, it is commonly assumed that self-centering will be achieved if the moment provided by the energy dissipating elements was less than the moment provided by the PT (Stanton *et al*. 1997). This concept is referred to as "static self-centering", where the flag-shaped hysteresis response is assumed to pass through the origin.

The bi-linear elastic hysteresis assumption may be valid for some previously tested PT systems up to certain drift limits, but it is seldom achieved for PT concrete members with realistic design parameters. Cyclic tests on both unbonded PT concrete frames (Palmieri *et al*. 1997) and concrete walls (Perez *et al*. 2003) have indicated that the response of the PT concrete member included noticeable stiffness degradation and cyclic hysteresis area, as shown in Fig. 2(a). This imperfect bi-linear elastic hysteresis response, which is caused by inelastic strains in the compression toe of the concrete member, increases the residual drift observed in the cyclic hysteresis response. This deviation from the idealised behaviour was further highlighted during tests of self-centering concrete systems (Stanton *et al*. 1997, Priestley *et al*. 1999, Restrepo and Rahman 2007, Sritharan
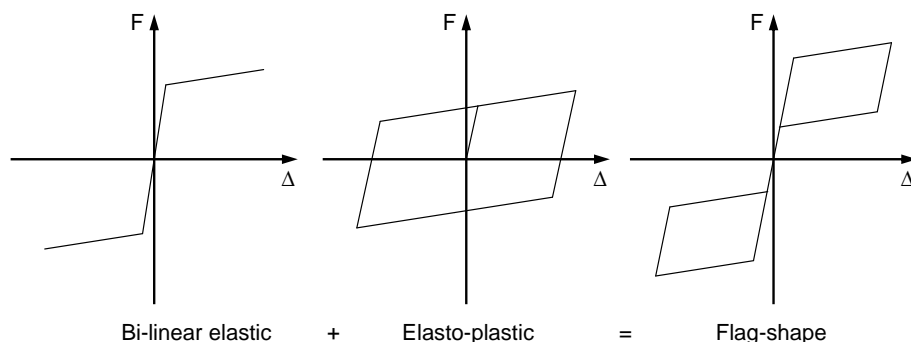

Bi-linear elastic   +   Elasto-plastic   =   Flag-shape
Fig. 1 Idealised flag-shape hysteresis response typically assumed for self-centering concrete systems

(a) PT wall (Perez et al. 2003)   (b) Jointed wall (Priestley et al. 1999) (c) PreWEC (Sritharan et al. 2008)
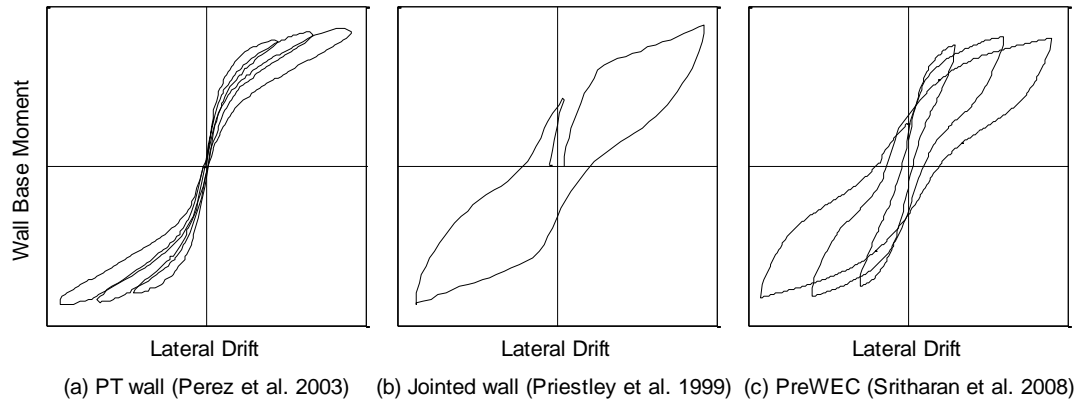
Fig. 2 Extracted hysteresis responses from previous wall tests

et al. 2015), as shown in Fig. 2(b) for the jointed wall system and in Fig. 2(c) for the PreWEC system. The inelastic strains in the wall toe can be minimised by either modifying the wall design or armouring the wall toe, but for walls with a significant prestress force the imperfect hysteresis shape is difficult to avoid. The PreWEC wall system tested by Sritharan *et al*. (2015) included steel channels to armour the wall toes and subsequent damage to this armour may have contributed to the observed hysteresis response.

A similar imperfect flag-shaped response with stiffness degradation was observed by Chou and Hsu (2008) for PT segmental bridge columns. Chou and Hsu proposed a stiffness degrading flag-shape hysteresis rule that was able to better capture the hysteresis response of experimentally tested PT columns. However, the proposed model did not include allowance for small residual drifts in the cyclic hysteresis response, such as those presented in Fig. 2. Alternatively, more sophisticated models of PT concrete members have been used that can capture both the stiffness degradation and residual drifts, such as the fibre-element models (Kurama 2002), multi-spring models (Pampanin *et al*. 2010), and finite element models (Henry 2012).

In addition to using an idealised hysteresis response for the self-centering system, the interaction with other structural and/or non-structural elements in a building is not given any consideration. For self-centering concrete wall systems, that the inclusion of additional structural and non-structural elements (such as wall-to-floor interaction) has been shown to drastically alter the system's hysteresis behaviour, with an increase in strength, energy dissipation and residual drift (Henry *et al*. 2012). The influence of gravity framing and non-structural systems on the seismic response of self-centering steel rocking systems has also been investigated by Eatherton and Hajjar (2011). Therefore, even if the main lateral load resisting system has self-centering ability, the entire structure may not completely recenter, which defeats the purpose of using self-centering seismic resistant systems in buildings.

2.2 Current design procedures

Despite the experimentally observed behaviour and sophisticated modelling approaches recommended for PT concrete members, current design procedures that are used to ensure that self-centering is achieved are predominantly based upon the ideal flag-shaped hysteresis response.

As a result of the PRESSS research program, ACI design guidelines for self-centering concrete frames included the expression shown in Eq. (1), which states that the moment contribution from energy-dissipating reinforcement, M_s, must equate to less than 50% of the probable flexural strength of the member, M_{pr}. In accordance with capacity design procedures, the New Zealand concrete design standard adopted a similar expression that also included an overstrength factor for the energy dissipating components. The equation included in Appendix B of NZS 3101:2006 is shown in Eq. (2), where the moment contribution ratio, λ, must be greater than the overstrength factor of the energy dissipating components, α_o, where M_{pt} is the moment provided by the unbonded PT and M_N is the moment provided by additional axial load (including self-weight). In New Zealand, the overstrength factor for mild steel is typically 1.15 or greater (NZS 3101:2006), which implies that the moment contribution from the energy dissipating components should be less than 46% of the total flexural strength. The design guidelines for self-centering concrete systems published by the New Zealand Concrete Society (Pampanin *et al*. 2010) also includes Eq. (2), but it is further recommended that the moment provided by the energy dissipating components should not exceed 40% of the total moment resistance

$$\frac{M_s}{M_{pr}} \leq 0.5 \tag{1}$$

$$\lambda = \frac{M_{pt} + M_N}{M_s} \geq \alpha_o \tag{2}$$

The ACI Innovation Task Group 5 (ITG-5) that established the code requirements for the development and design of unbonded post-tensioned concrete walls did not include a specific procedure to ensure that self-centering was achieved. However, ITG-5.1 (2007) states that studies by Kurama (2002) indicated that the self-centering capability following a major earthquake may be lost if more than 40% of the flexural capacity was provided by energy dissipating elements.

Both Eqs. (1) and (2) are intended to be calculated at the design lateral drift, or ultimate moment resistance, which is not sufficient to ensure static self-centering of the cyclic hysteresis loops, as demonstrated later in Section 3. Additionally, Eqs. (1) and (2) do not account for realistic cyclic or dynamic hysteresis behaviour, when considering the self-centering capability of an entire structure during an earthquake.

2.3 Dynamic self-centering

A residual displacement observed from a cyclic hysteresis loop does not necessarily guarantee poor building performance. This is because the residual drift of a structure subjected to an earthquake depends on the peak drift that the structure experiences, as well as its dynamic response during the remainder of the earthquake duration and the free vibration that occurs at the end of an earthquake input motion. This post-peak behaviour, referred to as the "shake-down" phenomenon (MacRae and Kawashima 1997), is illustrated in Fig. 3. As a result, the residual drift at the end of dynamic response, d_r, will typically be less than the maximum residual drift immediately following the peak lateral drift, $d_{r,max}$.

After recognising that the residual drift of a structure was a function of the hysteresis behaviour and the earthquake ground motion, MacRae and Kawashima (1997) conducted a series of dynamic
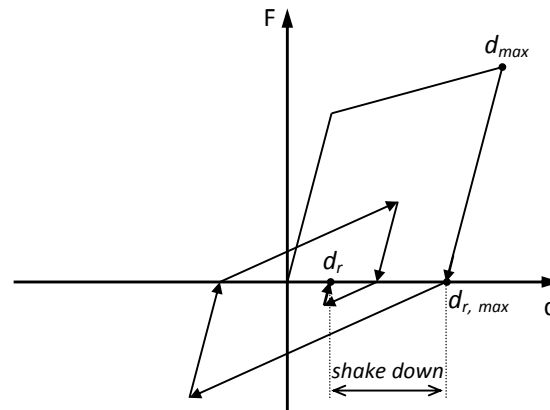
Fig. 3 Dynamic shake-down behaviour [adapted from Christopoulos *et al*. (2003)]

analyses to investigate the behaviour of single-degree-of-freedom oscillators. MacRae and Kawashima found that even for oscillators with elasto-plastic hysteresis rules, significant reduction in the residual displacement was observed due to the shake-down effect. The residual displacement at the end of the ground motion was normalised by the maximum possible residual displacement to define the residual displacement ratio (d_{rr}).

Residual drifts were also the focus of a performance based assessment of frame structures that was conducted by Christopoulos *et al*. (2003). Christopoulos et al. carried out a series of dynamic single-degree-of-freedom analyses to compare the seismic response of systems having elasto-plastic, Takeda, and flag-shape hysteresis rules. Although noting that dynamic shake-down reduced the residual drifts of the elasto-plastic and Tekada systems, Christopoulos *et al*. argued that the full benefit of self-centering systems could not be assessed without considering the residual drifts. However, it should be noted that because an ideal flag-shape hysteresis rule was used during the analyses, a realistic assessment of the residual drifts observed in self-centering systems was not established by Christopoulos *et al*.

3. Analysis of flag-shape response

Although self-centering concrete systems exhibit a response that appears flag-shaped, the idealised flag-shape representation shown in Fig. 1 does not typically exist for two reasons. First, the responses of the PT member and energy dissipating components cannot be simply added together because energy dissipating elements are only engaged after decompression followed by uplift at the tension toe. Second, an imperfect flag-shape is achieved when realistic hysteresis responses are used for both the PT member and the energy dissipating elements. A series of cyclic analyses were conducted to demonstrate that the current self-centering design procedures can be inaccurate even when idealised hysteresis models were adopted and the dynamic shake-down effects were ignored.

3.1 Lumped plasticity model

The response of an idealised self-centering concrete system can be captured using a lumped

plasticity model (Palermo *et al.* 2007). The structural member (wall, column, or beam) is represented by an elastic beam member, with the non-linear behaviour lumped into two rotational springs at the base of the member. The two rotational springs represent the base moment-rotation behaviour of the PT member and energy dissipating components, respectively. This type of lumped plasticity model is suitable for cantilever type members where axial elongation is not prevented.

3.2 Cyclic analysis

To analyse the flag-shaped hysteresis behaviour, a two-spring lumped plasticity model was constructed using the non-linear structural analysis program Ruaumoko (Carr 2003). The model properties were approximately defined based on a self-centering concrete wall test specimen known as PreWEC (Sritharan *et al.* 2015). The intention of the analysis was not to match or compare the PreWEC wall response exactly, but to define a simple spring model to investigate the flag-shape hysteresis and self-centering criteria previously described. The model consisted of a 6.1 m tall elastic beam element with an EI equal to 3230 Nmm^2 to represent the wall. The rotational springs were designed to approximately match the 3000 kNm wall base moment and the top of the beam member was subjected to a single lateral displacement cycle to 2.5% drift.

The first analysis was conducted using idealised hysteresis models for the rotational springs, including a bi-linear elastic definition for the PT spring and a bi-linear elasto-plastic definition for the energy dissipation (ED) spring. As shown in Fig. 4(a), both rotational springs had equal yield moments of 1250 kN-m and ultimate moments of 1500 kN-m (corresponding to approximately 2.5% lateral wall drift). The moment-drift response of the model, shown in Fig. 4(a), indicated that the flag-shaped response consisted of five distinct segments. When compared to the idealised flag-shape that was shown in Fig. 1, the initial stiffness consisted of two segments due to the different yield rotations of the PT and ED springs. It should be noted that this observation is consistent with previous results published for such systems. First, the stiffness of the system is controlled by the elastic response of the wall, but once decompression occurs at the wall toe, the stiffness is then influenced by the second slope of the PT spring and the initial stiffness of the energy dissipating spring. Upon unloading, the hysteresis response returned to the origin with zero residual drift. Using current self-centering procedures described previously, a zero residual drift would be expected because the moment attributed to the energy dissipating components did not exceed the moment attributed to the PT.

For the second analysis, the post-yield stiffness of the ED spring was increased, so that the ultimate moment of the ED spring exceeded that of the PT spring, as shown in Fig. 4(b). Interestingly, as observed from Fig. 4(b), the resulting moment-drift hysteresis response of the system exhibited perfect self-centering with zero residual drift after unloading. This observation demonstrated that the traditional criterion that was used to ensure self-centering occurred was inaccurate and ambiguous, as perfect static self-centering was achieved even when the energy dissipating components provided more than 50% of the total moment. Although there is some correctness to the 50% ED moment criteria, the point at which this calculation is performed during the response is critical. As previously stated, the proportion of the moment provided by the energy dissipating components at the maximum lateral drift is not relevant, and instead the moment balance calculation should be performed based on the strength of the energy dissipating element when the spring returns to zero rotation. Although the traditional criterion used to ensure self-centering described previously in Eq. (1) and Eq. (2) could be expressed in terms of the strengths
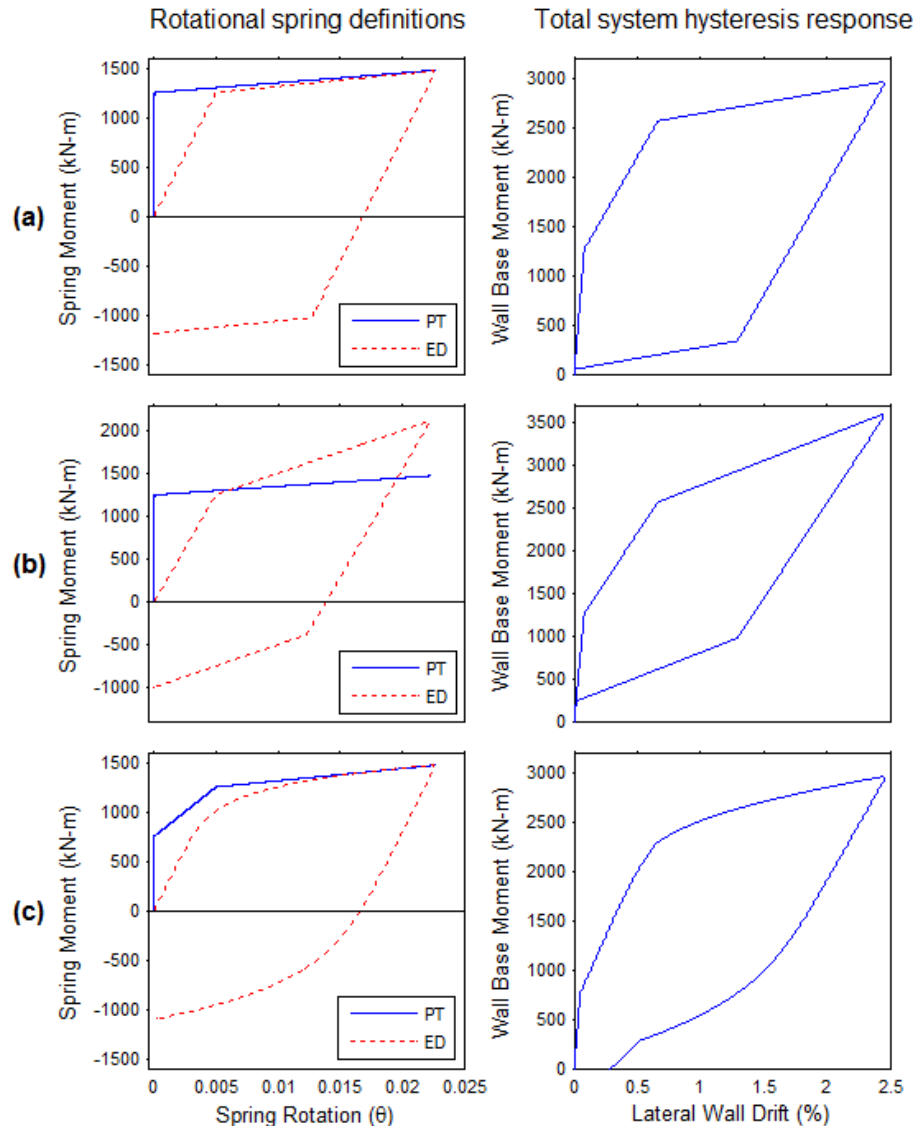
Fig. 4 Two spring lumped plasticity model with idealised hysteresis and equal moment resistance

at zero rotation, the rules would still be based on idealised hysteresis definitions and may not capture the true self-centering ability.

As discussed previously, hysteresis definitions of the PT and ED rotational springs in realistic self-centering systems do not perfectly follow the bi-linear elastic and bi-linear elasto-plastic rules. The backbone response of an undamaged PT member (ignoring the wall hysteresis energy dissipation) can be more accurately approximated using a tri-linear elastic hysteresis (Aaleti and Sritharan 2008), while the energy dissipating components typically display a smoother elasto-plastic hysteresis response. For the third analysis, a tri-linear elastic definition was used for the PT

spring and a Ramberg-Osgood definition was used for the ED spring with a bi-linear actor (r) of 7.4, as shown in Fig. 4(c), and the yield moments and ultimate moments of the PT and ED springs were approximately equal. As shown in Fig. 4(c) the resulting hysteresis response deviated from the ideal flag-shape behaviour, with a more realistic smooth form that is consistent with that shown previously in Fig. 2. Although the moment provided by the energy dissipating components did not exceed the moment provided by the PT, perfect self-centering was not achieved and a small residual drift was observed. This residual drift was primarily attributed to the tri-linear PT spring and the reduction in the decompression moment. The use of the Ramberg-Osgood rule softened the edges of the curve, but did not significantly alter the self-centering behaviour. This analysis further highlighted that when considering the ability of the system to self-centering with zero residual drift, the PT and ED moment contributions are only critical when the springs are unloaded to zero rotation. In this case, the unloaded moment in the ED spring of -1100 kN-m exceeded the 750 kN-m yield moment of the PT spring and thus perfect static self-centering was not achieved.

4. Residual drift limits

As explained in previous sections and shown in Fig. 2, real self-centering concrete systems will typically exhibit some degree of residual drift even when traditional criteria (e.g., Eq. (1) and Eq. (2)) intended to ensure self-centering is satisfied. However, because the response follows an approximately flag-shaped behaviour, the residual drifts observed in a self-centering system are typically small when compared to those of traditional construction systems. Analyses preformed by Kurama (2002) using an accurate fibre model confirmed that due to the shake-down effect, the small residual drift observed from the cyclic hysteresis loops of hybrid walls led to almost zero residual drift during seismic excitation. If residual drifts still occur in real self-centering concrete systems, appropriate limits need to be set to define what is classified as self-centering behaviour.

To determine appropriate residual drift limits for a self-centering structure, target seismic performance levels must first be determined. Using performance based design principles, target performance levels can be linked to seismic hazard based on the design objective (Seismology Committee 1999). As shown in Fig. 5, the basic design objective using the prevailing ductile seismic design philosophy is intended to target a life-safety performance level when subjected to the design level earthquake (seismic hazard EQ-III) and prevent collapse when subjected to the maximum considered earthquake (seismic hazard EQ-IV). Resilient seismic design correlates to the enhanced objectives 1 and 2, where the damage caused to the structure during the design level and maximum considered earthquakes is reduced.

Using the enhanced objective 1 performance levels shown in Fig. 5, residual drift limits for self-centering concrete systems were established for each hazard level based on recommendations by Rahman and Sritharan (2006, 2007). This procedure resulted in the residual drift limits described in Table 1, with allowable permanent residual drift up to 10% of the target lateral drift equal to 0.2% following the design level earthquake and up to 0.3% following the maximum considered earthquake. It was considered that these residual drift levels provided realistic limits for seismic resilient buildings, resulting in sufficient recentering to allow for the building to be reoccupied following a major earthquake. It should also be noted that a residual drift of 0.2% aligns well with typical vertical construction tolerances implying that the building would still be functional.
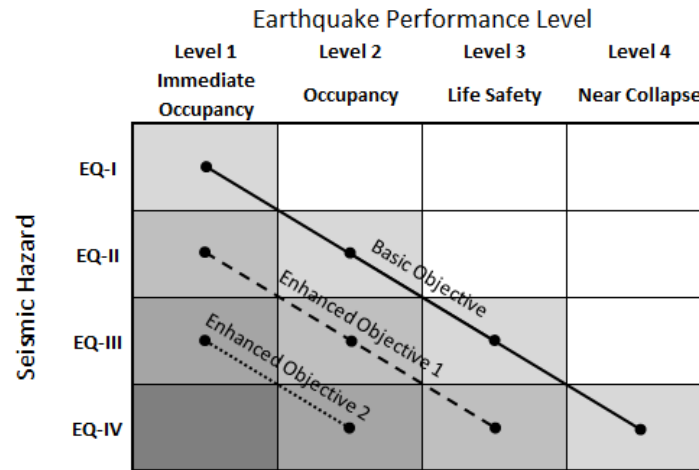
Fig. 5 Seismic performance objectives for buildings (Seismology Committee 1999)

Table 1- Residual drift performance limits for realistic self-centering systems

Seismic hazard	Residual drift limit (%)
EQ-I	0.1
EQ-II	0.1
EQ-III	0.2
EQ-IV	0.3

5. Dynamic analysis

To accurately assess the expected residual drifts of a structure following an earthquake, both the realistic cyclic hysteresis response and the dynamic shake-down need to be included. A series of dynamic time-history analyses were conducted to investigate the behaviour of realistic buildings with self-centering concrete walls when subjected to earthquake ground motions. The dynamic analyses utilised the PreWEC self-centering wall system that consists of a post-tensioned precast concrete wall with end columns and energy dissipating connectors (Sritharan *et al*. 2015).

5.1 Model development

A lumped plasticity model was developed to represent the PreWEC self-centering wall system using the non-linear dynamic structural analysis program Ruaumoko (Carr 2003). The wall was modelled using a beam element with a length equal to the height of the wall and was assigned an elastic hysteresis rule based on the uncracked elastic properties of the concrete wall and concrete filled steel tubular columns. The model used a total of seven non-linear rotational springs to represent the moment-rotation response at the base of the wall. The combination of seven rotational springs was carefully selected and calibrated to closely match the recorded hysteresis response of the PreWEC test specimen. Full details of the model development and properties of these seven rotational springs has been published by Henry (2011).

To investigate the accuracy of the lumped plasticity model, the top of the wall element was
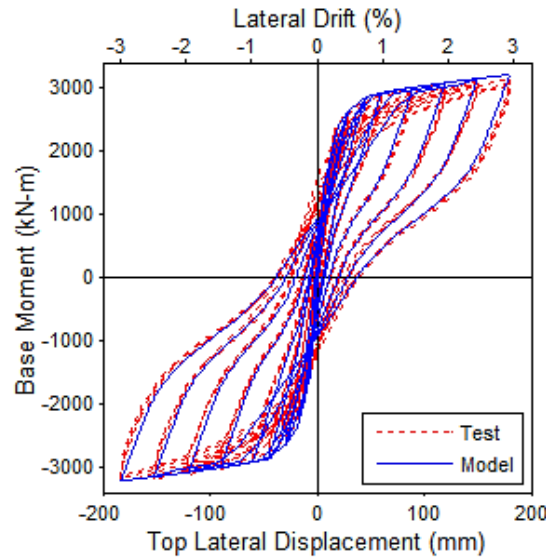
Fig. 6 Calculated cyclic response of the lumped plasticity model compared with the experimental results of the half-scale PreWEC specimen

subjected to the cyclic lateral displacement history that was measured during the PreWEC test (Sritharan *et al*. 2015). The results of the cyclic analysis of the lumped plasticity model are compared against the PreWEC experimental response in Fig. 6. It can be seen that the combination of rotational springs accurately captured the experimental response though all stages of the hysteresis loops. In particular the model accurately captured the unloading curve, residual displacement, and reloading stiffness degradation, which would not be captured if an idealised flag-shaped hysteresis rule was used.

5.2 Parametric matrix

In order to assess the seismic performance and permanent residual drift over a wide range of self-centering designs, an extensive parametric matrix was developed to vary the fundamental period of the structure, quantity of hysteretic energy dissipation, viscous damping, seismic hazard level, and earthquake ground motion.

5.2.1 Fundamental period / building height

The first set in the parametric matrix consisted of five single lumped mass models that were designed to represent buildings with heights equivalent to 2, 4, 6, 8 and 10 storeys, with an assumed inter-storey height of 3.66 m. For each of the five models, the lateral resistance was provided by a single PreWEC wall with cross-sectional dimensions and base moment-rotation behaviour equal to the full size equivalent of the PreWEC specimen that was previously tested at half-scale (Sritharan *et al*. 2015). Additional details of the scaling parameters are discussed by Henry (2011). The five models in the set were not intended to represent an increasing number of floors of the same floor-plan. Instead, each wall was designed with a tributary area (and mass) sufficient to impose a seismic demand that the PreWEC wall was designed to resist. This first set

Table 2 Properties of the five buildings designed

Wall	No. of storeys	Δ_d (m)	h_e (m)	V_b (kN)	K_e (kN-m)	T_e (s)	m_e (tonne)	T_i (s)
1	2	0.122	6.1	4066	33324	1.48	1860.3	0.38
2	4	0.220	10.98	2259	10285	2.67	1860.3	0.86
3	6	0.317	15.86	1564	4930	3.86	1860.3	1.46
4	8	0.415	20.74	1196	2883	5.05	1860.3	2.15
5	10	0.512	25.62	968	1889	6.24	1860.3	2.93

where Δ_d is the design lateral displacement at the effective height, h_e, V_b is the design base shear, K_e is the effective stiffness, T_e is the effective period, m_e is the effective mass, and T_i is the fundamental period

of five wall models is referred to as P_{test} to represent the PreWEC test specimen.

In order to design a range of different structures using the same PreWEC wall design, the building properties were back-calculated from the required base moment-rotation behaviour using the Direct Displacement Based Design (DDBD) procedure (Priestley *et al.* 2007). The walls were designed for a design level displacement (Δ_d) of 2% lateral drift, as recommended by the ACI ITG-5 documents (2007, 2009) and used by previous researchers (Priestley *et al.* 1999, Rahman and Sritharan 2006, Pennucci *et al.* 2009). At 2% lateral drift the base moment resistance of the full scale PreWEC wall was calculated to be 24,800 kN-m. The effective stiffness (K_e), period (T_e) and mass (m_e) of the SDOF representation of each structure was then back-calculated from this moment resistance with an assumed 3% elastic equivalent viscous damping, as recommended from previous research into self-centering concrete systems (Kurama 2002, Wight *et al.* 2004, Ma 2010). The exact site condition was not critical to the outcome of this investigation, so for the purpose of this study the buildings were located in California seismic Zone 4 on intermediate soil, S_c, as defined by SEAOC (Seismology Committee 1999). The properties of the resulting five wall designs are shown in Table 2. The 5 walls resulted in effective periods from 1.48 to 6.24 s.

5.2.2 Hysteretic energy dissipation

A further two sets of five walls that had a base moment-rotation behaviour with either more or less hysteresis area were included in the parametric study, referred to as P_{more} and P_{less}. The hysteresis behaviour was modified by multiplying the connector spring moments by a factor of 1.4 (14 connectors instead of 10) or 0.8 (8 connectors instead of 10), while the moment resistance of the six remaining springs that represented the post-tensioned wall behaviour were reduced or increased by the same factors respectively. These modified quantities of energy dissipating connectors resulted in equivalent viscous damping at the design level drift of 18.7% for P_{more} and 13.7% for P_{less}, compared to 15.3% for P_{test}. The modified hysteresis area could represent either increasing or reducing the number of energy dissipating connectors in the PreWEC system, or the influence of additional hysteretic energy dissipation provided by other structural and non-structural elements. The modified base moment-rotation behaviours were then applied to all five walls in the set shown previously in Table 2, providing an increased data set to assess the dynamic response and residual drift of a wide range of self-centering building designs.

5.2.3 Viscous damping

The influence of the assumed elastic equivalent viscous damping was also investigated. As

described above, 3% damping was assumed during the design and initial analytical investigation. Analyses for wall set P_{test} were repeated with 1% and 5% viscous damping to assess the sensitivity of the assumed elastic damping, as well as investigate any potential relationship between the elastic damping and the residual drift.

5.3 Earthquake records

The self-centering lumped plasticity model was subjected to a series of earthquake ground motions representing the design level (EQ-III) and maximum considered (EQ-IV) seismic hazard. All the ground motions used during this investigation were sourced from the PEER strong motion database (http://peer.berkeley.edu/smcat/).

5.3.1 Ground motion selection

A total of seven earthquake ground motions (GM) were selected for this investigation, with the details given in Table 3. The ground motion records were primarily sourced from previous studies (Christopoulos *et al*. 2002, Rahman and Sritharan 2007, Pennucci *et al*. 2009) and selected to represent a wide range of excitation that was expected for a high seismic zone and intermediate soil (S_c) condition around the world. Except for El Centro and Imperial Valley, all of the recording stations were located in USGS soil class B which corresponds to an intermediate soil class S_c as defined by SEAOC (Seismology Committee 1999). The El Centro and Imperial Valley recording stations were located on softer class C soil, but the records were still found to be compatible with the S_c response spectrum. It should be noted that the ground motion set is small and intended to provide understanding of the trends rather than definitive rules on self-centering.

Although no provision for near fault effects was included during the wall design, the Chi-Chi, Kobe, and Tabas ground motion records were identified during a study by Cox and Ashford (2002) to contain a strong velocity pulse. A strong velocity pulse was considered to have a greater chance of causing a significant residual drift, by reducing the self-centering ability during dynamic shake-down.

5.3.2 Ground motion scaling

The earthquake acceleration records were scaled to match the 5% damped response spectrum for California seismic zone 4, soil type S_c, and seismic hazard levels EQ-III and EQ-IV. The

Table 3 Summary of earthquake ground motions (GM)

GM	Earthquake	Year	M_W	Station	Direction	Soil (USGS)	Distance (km)	PGA (g)	PGV (m/s)
1	Chi-Chi	1999	7.6	CHY080	NS	B	6.95	0.902	1.024
2	El Centro	1940	7	El Centro Array	EW	C	8.3	0.215	0.302
3	Imperial Valley	1979	6.5	Cucapah	85°N	C	23.6	0.309	0.363
4	Kobe	1995	6.9	KJMA	NS	B	0.6	0.821	0.813
5	Northridge	1994	6.7	Coldwater Can	EW	B	14.6	0.271	0.222
6	Northridge	1994	6.7	Mt Gleason Ave	NS	B	17.7	0.127	0.138
7	Tabas	1978	7.4	Tabas	LN	B	1.2	0.836	0.978

M_W is the moment magnitude, PGA is the peak ground acceleration, and PGV is the peak ground velocity

Table 4 Scale factors for earthquake ground motions

Hazard level	Wall	Ground motion						
		GM-1	GM-2	GM-3	GM-4	GM-5	GM-6	GM-7
		Chi-Chi	El Centro	Imperial	Kobe	N-Ridge 1	N-Ridge 2	Tabas
EQ- III	1	0.47	1.85	1.71	0.43	1.87	3.01	0.64
	2	0.7	1.75	1.6	0.77	1.92	3.53	0.6
	3	0.97	1.73	1.81	1.13	1.92	3.63	0.62
	4	0.99	1.78	2.2	1.4	2.11	4.54	0.62
	5	1.08	2.01	2.64	1.53	2.32	4.41	0.66
EQ-IV	1	0.7	2.78	2.57	0.64	2.8	4.51	0.96
	2	1.05	2.62	2.4	1.15	2.88	5.29	0.89
	3	1.45	2.59	2.71	1.69	2.88	5.44	0.93
	4	1.49	2.68	3.3	2.1	3.17	6.81	0.94
	5	1.62	3.01	3.95	2.29	3.48	6.61	1

scaling was performed as outlined by the SEAOC guidelines (Seismology Committee 1999), which included minimising the sum of the squared difference between spectral ordinates, while also ensuring that all spectral ordinates were at least 70% of the design response spectrum. This scaling procedure was conducted for each of the five walls in the design set, with the response spectrum matched between the fundamental period, T_i, and the effective period, T_e. The calculated scale factors used during the analyses are summarised in Table 4.

5.4 Analysis details

The dynamic time-history analyses were conducted using the lumped plasticity model described in section 5.1. The analyses were conducted using the lumped mass, or SDOF representation, that was used during the DDBD design process. The entire effective mass, m_e, was located at the top node of the wall element, which had a length equal to the effective wall height, h_e. No gravity or static loads were applied to the model because the moment-rotation behaviour of the base springs was defined to include the effect of the wall self-weight. The analyses used an integration time step of 0.001s with the Newmark constant average acceleration solution method. As described above, 3% initial stiffness proportional Rayleigh viscous damping was used in the model. The horizontal earthquake ground motions were applied separately to the structure and all nodes were restrained from movement in the out-of-plane direction. Additionally, the nodes between the rotational springs, and at the bottom of the wall beam member, were constrained to allow only in-plane rotation to occur. The analysis time was equal to the full length of the ground motion record plus a free vibration time that was equal to at least $20T_i$. The free vibration time allowed the structure sufficient time for the response to decay completely, allowing accurate calculation of the final residual drift.

5.5 Analysis results and discussion

A summary of the results from the 350 analyses conducted during the parametric investigation

are discussed in this section. These analyses consistent of the 70 cases listed in Table 4 multiplied by the 3 different sets P_{test}, P_{more}, P_{less}, in addition to P_{test} repeated at 1% and 5% elastic damping. Full results of all of the analyses are discussed in more detail by Henry (2011).

5.5.1 Maximum drift

For the design wall set P_{test}, the calculated maximum lateral drift results from the time-history analyses correlated well with the design target drift levels for both hazard levels EQ-III (DBE) and EQ-IV (MCE). The average maximum drift calculated for each of the five walls was between 1.85% and 2.11% drift for the DBE ground motions compared to a 2% design target drift, and between 2.62% and 3.36% drift for the MCE ground motions compared to a 3% target drift. These results highlighted the accuracy of the displacement based design process used to construct the wall matrix. Although some of the earthquake ground motions could be considered to include near-fault effects, the dominant velocity pulse in each ground motion was typically only noticeable for one of the five walls. When the frequency of the earthquake's velocity pulse matched the fundamental period of the wall a large pulse was observed in one direction. However, no single earthquake caused a large pulse response for all five walls.

The analyses of the wall sets with more and less hysteretic energy dissipation, P_{more} and P_{less}, resulted in average maximum lateral drifts that were higher and lower than the 2% design target drift respectively. This result was expected because the increased and decreased hysteretic energy dissipation was not accounted for during the direct displacement based design procedure, with the wall designs based on the P_{test} hysteresis behaviour.

5.5.2 Residual drift

The main objective of the analytical investigation was to investigate the residual drift that the system exhibited following the ground motion. The calculated residual drifts for wall sets P_{test}, P_{more} and P_{less} with 3% equivalent viscous damping are shown in Fig. 7 for hazard levels EQ-III and EQ-IV. For all P_{test} analyses, the residual drift was below the corresponding permissible limits that were defined in section 4. For the design hazard level EQ-III, the residual drift limit of 0.2% was not exceeded and the average residual drift was approximately 0.05%. Additionally, the 0.3% residual drift limit set for the maximum considered earthquake, corresponding to hazard level EQ-IV, was never exceeded during any of the analyses. These results confirmed that the designed PreWEC system met the performance based assessment criteria to be classified as a seismic resilient or self-centering structure.

When compared to the design wall set P_{test}, the average residual drifts were higher for wall set P_{more} and lower for wall set P_{less}. The increase and decrease in the average residual drift was due to the change in the residual drift observed in the cyclic hysteresis loops with more and less hysteretic energy dissipation. Two analyses from the P_{more} wall set and one analysis from the P_{less} wall set resulted in a calculated residual drift that slightly exceeded the residual drift performance limit of 0.2% for the design level earthquake intensity by up to 12.5%. This observation confirms that while DDBD produces satisfactory design outcomes, it is somewhat sensitive to the assumed level of damping and target drift used for the design.

The calculated residual drift did not display any significant trend with regard to the natural period (wall number), or the earthquake ground motion. As seen in Fig. 7, the average residual drift was relatively constant across all wall designs. Interestingly, some of the analyses that exhibited an outlying maximum drift and an asymmetrical response, that may have been considered a consequence of a strong velocity pulse, did not result in large residual drifts. For
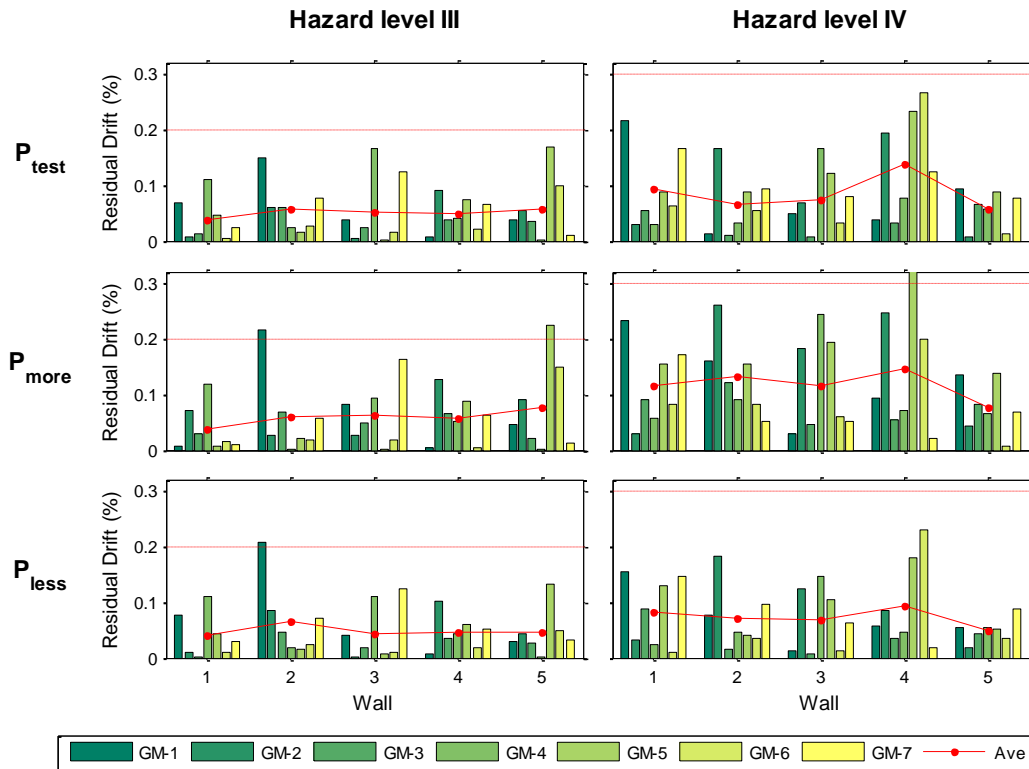
Fig. 7 Residual drift results from the dynamic analyses

example, for P_{test} hazard level EQ-IV, GM-3 for wall 1 and GM-5 for wall 2 both exhibited maximum drifts in excess of 4% drift, but neither had a residual drift larger than 0.1%. Despite a large pulse in one direction the subsequent smaller load cycles were sufficient to recenter the wall. This finding highlighted the significance of the shake-down effect, and the ability of the PreWEC hysteresis behaviour to self-center during a small load reversal that followed the peak lateral displacement.

5.5.3 Residual drift ratio

To quantify the effectiveness of the shake-down effect and to develop a non-dimensional design parameter, the residual drift ratio that was utilised by MacRae and Kawashima (MacRae and Kawashima 1997) was examined. The residual drift ratio, d_{rr}, was calculated by dividing the residual drift at the end of the analysis, d_r, by the maximum possible residual drift, $d_{r,max}$, which is the residual drift when unloading immediately following the maximum lateral displacement (also referred to as maximum static or cyclic residual drift).

The calculated residual drift ratios for all analyses in sets P_{test}, P_{more}, and P_{less} with 3% equivalent viscous damping are plotted against the maximum possible residual drift in Fig. 8. The highest residual drift ratio was calculated to be 0.44, which means that the shake-down effect reduced the residual drift to less than 44% of the maximum possible residual drift. This reduction confirmed that self-centering should not be exclusively defined from the peak cyclic hysteresis loops, but that the residual drift following an earthquake is equally important during design.
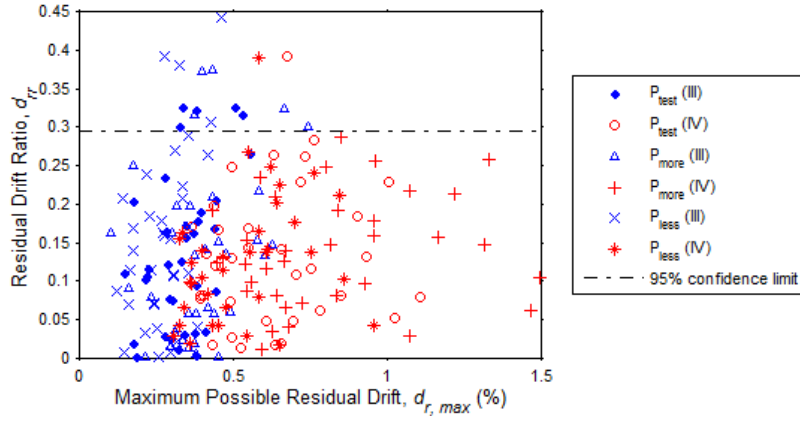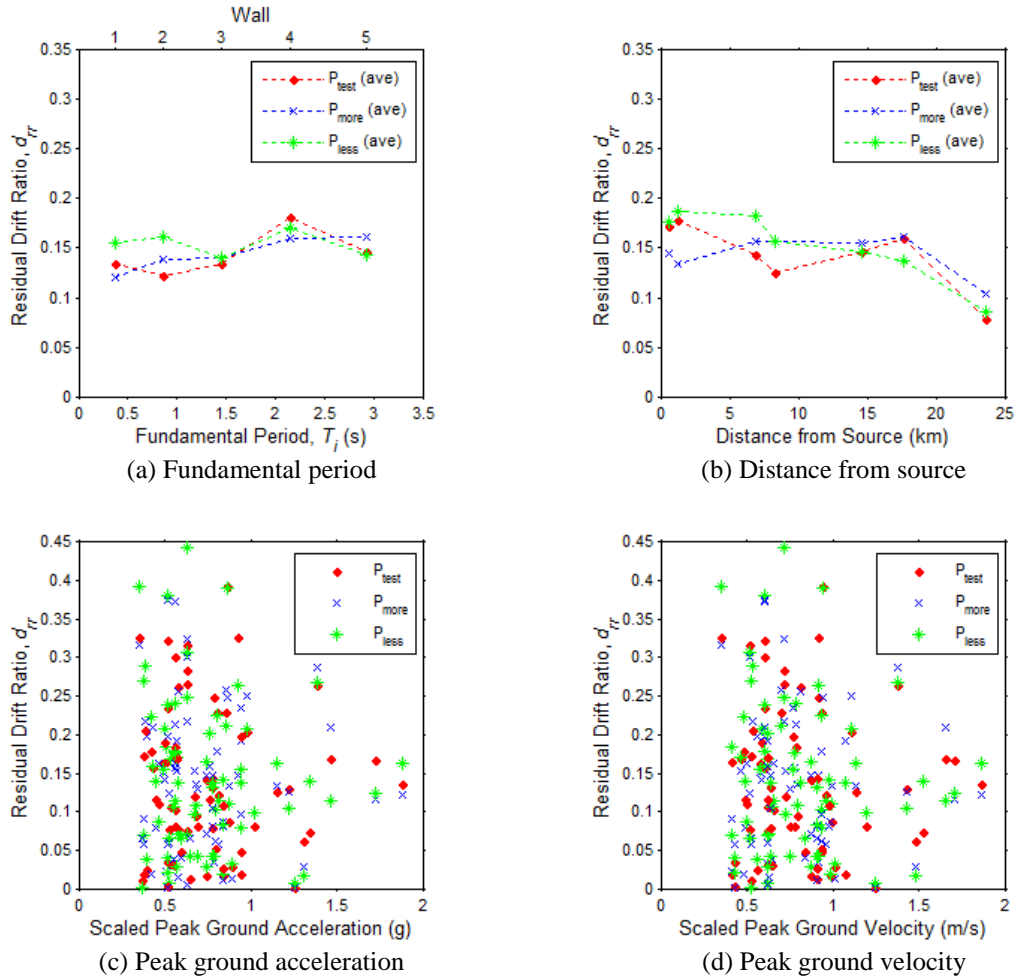
Fig. 8 Residual drift ratio for wall sets P_{test}, P_{more} and P_{less}

(a) Fundamental period

(b) Distance from source

(c) Peak ground acceleration

(d) Peak ground velocity

Fig. 9 Influence of fundamental period and ground motion parameters on the residual drift ratio

However, there is considerable scatter in the residual drift ratio, which appeared to be due to variations in the characteristics of ground motions, including duration, symmetry, and the decay in intensity.

The residual drift ratio can be used as an important design tool for assessing the maximum predicted residual drift. A 95% upper bound confidence limit equal to 0.295 was established from the residual drift ratio data, as shown in Fig. 8. This confidence limit was rounded to 0.3 to provide an appropriate upper limit for the residual drift ratio that could be used during design of buildings with PreWEC walls. However, there was significant scatter observed in the results and more in-depth investigation was conducted in search of variables that influenced the residual drift ratio.

To investigate the relationship between fundamental period and the residual drift ratio, the average residual drift ratio was calculated for each wall in sets P_{test}, P_{more}, and P_{less}. As seen in Fig. 9(a), the residual drift ratio showed no significant trend as the fundamental period increased, with only minor inconsistent variations observed. Additionally, no significant difference was observed between the analysis sets with different hysteretic energy dissipation.

The influence of the ground motion parameters on the residual drift ratio was also investigated. The residual drift ratio for all analyses in sets P_{test}, P_{more}, and P_{less} are plotted in Fig. 9 against the ground motion distance from the source, peak ground acceleration, and peak ground velocity. The average residual drift ratio for each ground motion also exhibits a slightly decreasing trend with respect to the distance from the earthquake source. Both the scaled peak ground acceleration and the peak ground velocity showed large scatter, with no significant correlation observed with the residual drift ratio.

5.5.4 Assumed viscous damping

As explained earlier, the analyses for wall set P_{test} were repeated with 1% and 5% viscous damping to assess the effect of the assumed elastic viscous damping. As expected, when 1% damping was used for the analyses, the average maximum drifts for each wall were higher than the 2% design target, while the average maximum drifts for the 5% damping analyses were below the 2% design target. Most importantly, the effect of the elastic damping selection on the residual drift ratio was investigated. A similar trend was observed to the design analyses conducted with 3% viscous damping, with all calculated residual drift ratios being below 0.40. The 95% confidence limit for the 1% and 5% damping analyses was calculated to be 0.281. This calculated confidence limit was just below the 0.295 limit that was calculated for the 3% damping analyses and it was concluded that the assumed elastic damping did not appear to have any significant impact on the residual drift ratio.

6. Design procedure

As demonstrated by previous tests and the numerical analysis conducted, small residual drifts occur in realistic self-centering concrete wall systems. A modification to the traditional self-centering criteria is required to ensure that the resulting residual drifts are below acceptation limits. After analysing the results from the dynamic analyses described above, a procedure for a simple design check was established to include a residual drift limit in performance based design of self-centering systems. The steps involved in this procedure are summarised below:

• *Step 1:* Establish suitable residual drift performance limits. For self-centering concrete systems the suggested limits are 0.2% for the design hazard level (EQ-III) and 0.3% for the

maximum considered hazard level (EQ-IV).

    • <u>*Step 2:*</u> Complete preliminary design of the structure using force-based or displacement-based design.

    • <u>*Step 3:*</u> Based on published research or guidelines for the selected building system, estimate the maximum possible residual drift, $d_{r,max}$, corresponding to the design target drift at each performance level.

    • <u>*Step 4:*</u> Estimate the upper bound residual drift ratio, d_{rr}, which is equal to 0.3 for the PreWEC system based on the dynamic analyses presented.

    • <u>*Step 5:*</u> Multiply $d_{r,max}$ by d_{rr} to calculate the upper limit of the design residual drift, $d_{r,design}$.

    • <u>*Step 6:*</u> Check if $d_{r,design}$ is below the residual drift performance limit for each hazard level. If not, revise the design accordingly.

7. Implications for other systems

Although the dynamic analyses concentrated on the PreWEC concrete wall system, it is considered that the hysteresis behaviour is typical of realistic self-centering concrete wall systems. For instance, similarly shaped hysteresis behaviour was observed for the jointed wall system during the 5 storey PRESSS building test (Priestley *et al*. 1999). However, further analysis need to be conducted to determine the residual drift ratio suitable for different self-centering structural systems. When developing self-centering systems using any material or structural form, researchers should provide guidelines that enable calculation of both the realistic hysteresis response and the residual drift ratio so that the design procedure described in section 6 can be implemented.

8. Conclusions

Although the term self-centering is typically applied to any structure designed with unbonded PT, limited research has been conducted to investigate how self-centering is defined and the magnitude of residual drifts that occur in realistic concrete systems with unbonded PT. The validity of current design procedures was examined, and a parametric study was performed to investigate dynamic self-centering behaviour using the PreWEC concrete wall system as an example.

Based on the static and dynamic analyses conducted the following conclusions were made:

1. The current procedures that are used to ensure that self-centering occurs in concrete structures with a combination of unbonded PT and energy dissipating elements are inaccurate even when idealised hysteresis responses are assumed. Analyses showed that these current procedures could result in both conservative and unconservative estimates of the structure's self-centering ability.

2. To accurately ensure that self-centering is achieved when the structure is subjected to an earthquake, the realistic hysteresis response needs to be accounted for as well as the effects of dynamic self-centering. In real self-centering concrete systems, inelastic strains in the compression toe lead to a response that includes additional hysteretic energy dissipation, stiffness degradation and residual drift.

3. Residual drifts occur in real self-centering systems and appropriate performance limits need

to be established. It is recommended that for self-centering concrete buildings residual drifts should be limited to 0.2% following a design level earthquake and 0.3% following a maximum considered earthquake.

4. Time-history analyses of a lumped mass SDOF system showed that the residual drifts of an example self-centering concrete wall system at the conclusion of an earthquake were much lower than the maximum possible residual drift observed from the cyclic hysteresis loops, due to dynamic shake-down. As a result, the PreWEC wall system was found to meet performance based residual drift limits that could be used to define realistic self-centering behaviour.

5. A residual drift ratio was established to define the dynamic shake-down behaviour. No significant correlation was observed between the residual drift ratio and the fundamental period, hysteretic energy dissipation, the ground motion parameters, or the assumed viscous damping. The lack of obvious trends implied that the upper bound confidence limit for the residual drift ratio could be used during the design process. Based on the results of the analyses conducted an upper bound residual drift ratio of 0.3 could be used PreWEC wall system. However, additional analyses need to be conducted to refine the residual drift ratio suitable for a range of systems.

6. A simplified design process to incorporate a check on the estimated residual drift can be included during the design process. Although the analysis was performed using the PreWEC concrete wall system as an example, the results and design method are also applicable to other self-centering systems that have similar hysteresis behaviour.

Acknowledgements

References

Aaleti, S. and Sritharan, S. (2009), "A simplified analysis method for characterizing unbonded post-tensioned precast wall systems", *Eng. Struct*., **31**(12), 2966-2975.

ACI Innovation Task Group 5 (2007), "Acceptance criteria for special unbonded post-tensioned precast structural walls based on validation testing (ITG 5.1-07)", American Concrete Institute, Farmington Hills, MI.

ACI Innovation Task Group 5 (2009), "Requirements for Design of a Special Unbonded Post-Tensioned Precast Shear Wall Satisfying ACI ITG-5.1 (ITG 5.2-09)", American Concrete Institute, Farmington Hills, MA.

Carr, A. (2003), RUAUMOKO - Inelastic Dynamic Analysis Program, University of Canterbury, Christchurch, New Zealand.

Chou, C.-C. and Hsu, C.-P. (2008), "Hysteretic model development and seismic response of unbonded post-tensioned precast CFT segmental bridge columns", *Earthq. Eng. Struct. Dyn*., **37**(6), 919-934.

Christopoulos, C., Filiatrault, A. and Folz, B. (2002), "Seismic response of self-centring hysteretic SDOF systems", *Earthq. Eng. Struct. Dyn*., **31**(5), 1131-1150.

Christopoulos, C., Pampanin, S. and Priestley, M.J.N. (2003), "Performance-based seismic response of

frame structures including residual deformations. Part I: Single-degree of freedom systems", *J. Earthq. Eng*., **7**(1), 97-118.

Cox, K.E. and Ashford, S.A. (2002), "Characterization of large velocity pulses for laboratory testing", PEER 2002/22, Pacific Earthquake Engineering Research Center, Berkeley, CA.

Eatherton, M.R. and Hajjar, J.F. (2011), "Residual drifts of self-centering systems including effects of ambient building resistance", *Earthq. Spectra*, **27**(3), 719-744.

Henry, R.S. (2011), "Self-centering precast concrete walls for buildings in regions with low to high seismicity", Ph.D. thesis, University of Auckland, Auckland.

Henry, R.S., Aaleti, S., Sritharan, S. and Ingham, J.M. (2012), "Seismic analysis of a low-damage Precast Wall with End Columns (PreWEC) including interaction with floor diaphragms", *J. Struct. Eng. Soc. NZ. (SESOC)*, **25**(1), 69-81.

Kurama, Y.C. (2002), "Hybrid post-tensioned precast concrete walls for use in seismic regions", *PCI J*., **47**(5), 36-59.

Ma, Q.T. (2010), "The mechanics of rocking structures subjected to ground motions", Ph.D. thesis, University of Auckland, New Zealand.

MacRae, G.A. and Kawashima, K. (1997), "Post-earthquake residual displacements of bilinear oscillator", *Earthq. Eng. Struct. Dyn*., **26**(7), 701-716.

NZS 3101:2006 Concrete Structures Standard. Wellington, New Zealand, Standards New Zealand**:** 646.

Palermo, A., Pampanin, S. and Marriott, D. (2007), "Design, modeling, and experimental response of seismic resistant bridge piers with posttensioned dissipating connections", *J. Struct. Eng*., **133**(11), 1648-1661.

Palmieri, L., Sagan, E., French, C. and Kreger, M. (1997), "Ductile connections for precast concrete frame systems", *Mete A. Sozen Symposium, ACI SP 162*, American Concrete Institute, Farmington Hills, MI.

Pampanin, S., Marriott, D. and Palermo, A. (2010), *PRESSS design handbook*, Auckland, New Zealand Concrete Society.

Pennucci, D., Calvi, G.M. and Sullivan, T.J. (2009), "Displacement-based design of precast walls with additional dampers", *J. Earthq. Eng*., **13**(S1), 40-65.

Perez, F. J., R. Sause and L. W. Lu (2003). "Lateral load tests of unbonded post-tensioned precast concrete walls", *ACI Special Publication*, **211**, 161-182.

Priestley, M.J.N., Calvi, G.M. and Kowalsky, M.J. (2007), *Displacement-based seismic design of structures*, IUSS Press.

Priestley, M.J.N., Sritharan, S., Conley, J.R. and Pampanin, S. (1999), "Preliminary results and conclusions from the PRESSS five-story precast concrete test building", *PCI J*., **44**(6), 42-67.

Rahman, M.A. and Sritharan, S. (2006), "An evaluation of force-based design vs. direct displacement-based design of jointed precast post-tensioned wall systems", *Earthq. Eng. Eng. Vib*., **5**(2), 285-296.

Rahman, M.A. and Sritharan, S. (2007), "Performance-based seismic evaluation of two five-story precast concrete hybrid frame buildings", *J. Struct. Eng*., **133**(11), 1489-1500.

Restrepo, J.I. and Rahman, A. (2007), "Seismic performance of self-centering structural walls incorporating energy dissipators", *J. Struct. Eng*., **133**(11), 1560-1570.

Seismology Committee (1999), *Recommended lateral force requirements and commentary (Blue book)*, Structural Engineers Association of California (SEAOC), 327-421.

Sritharan, S., Aaleti, S., Henry, R.S., Liu, K.Y. and Tsai, K.C. (2015), "Precast concrete wall with end columns (PreWEC) for earthquake resistant design", *Earthq. Eng. Struct. Dyn*., **44**(12), 2075-2092.

Stanton, J., Stone, W.C. and Cheok, G.S. (1997), "A hybrid reinforced precast frame for seismic region", *PCI J*., **42**(2), 20-32.

Wight, G.D., Kowalsky, M.J. and Ingham, J.M. (2004), "Shake table testing of post-tensioned concrete masonry walls", RD-04-04, North Carolina State University, Raleigh, NC, USA.

KT